Noise Control Characteristics of Synchrophasing, Part 2: Experimental Investigation

James D. Jones* and C. R. Fuller†
Virginia Polytechnic Institute and State University, Blacksburg, Virginia

A simplified cylindrical model of an aircraft fuselage is used to investigate the mechanisms of interior noise suppression of the synchrophasing technique. This investigation allows isolation of important parameters to define the characteristics of synchrophasing. The optimum synchrophasing angle for maximum noise reduction is found for several interior microphone positions with pure tone source conditions. Noise reductions of up to 30 dB are shown for some microphone positions; however, overall reductions are less. A computer algorithm is developed to decompose the modal composition of the cylinder vibration over a wide range of synchrophase angles. The circumferential modal response of the shell vibration is shown to govern the transmission of sound into the cylinder rather than localized transmission.

Nomenclature

a = radius of test cylinder, 0.254 m
A_n, B_n = complex modal amplitude coefficients, Eq. (1)
f = frequency
j = $\sqrt{-1}$
m = $0,1,2,\ldots,\infty$
n = circumferential mode number
N_p = number of measuring points
p = $1,2,3,\ldots,N$
r,θ,x = cylindrical coordinates
t = time
w = radial displacement
$\Delta\theta_p$ = $2\pi/N_p$
ϵ = constant; $=2$ for $n=0$, $=1$ for $n>0$
ϕ = synchrophase angle
ω = circular frequency

Introduction

RECENTLY, interest has arisen over the use of advanced turboprop (ATP) engines in commercial aircraft, due to the potential of significant fuel savings. However, preliminary investigations have shown that the interior levels of the aircraft cabin exceed acceptable levels when ATPs are used. Several transmission paths for propeller noise in a wing-mounted configuration[1] have been identified. The dominant path for propeller noise appears to be the direct airborne path from the propeller blades through the cabin wall. Traditional passive techniques for noise control would require heavy damping material or additional mass around the propeller plane for the necessary noise reduction. The additional weight penalties for noise reduction would thus offset the potential fuel savings of ATP engines; therefore, it is beneficial to investigate alternative methods for interior noise reduction. As discussed by Metzger,[1] one of the most promising alternatives to passive techniques is synchrophasing. This technique involves synchronizing the relative rotational phase of the turboprop engines to achieve maximum interior noise reduction.

Promising results from previous experimental investigations[2,3] have been acquired during in-flight testing in an actual aircraft fuselage. However, this procedure will not allow the investigator to isolate individual parameters and correspondingly study their effect on synchrophasing. To date, the physical mechanisms behind the synchrophasing concept are not fully understood. In addition, the in-flight testing can be expensive and time consuming. Therefore, a cost-effective simplified procedure is needed to perform preliminary investigations of the characteristics of synchrophasing as well as other interior noise effects.

In this investigation, an experimental procedure was developed to study the mechanisms of synchrophasing utilizing a simplified model of an aircraft fuselage in a controlled environment. The model was designed to be simple enough to provide meaningful insights into transmission phenomena while describing the major physical mechanisms. The simplified model and sources used in this experimental investigation simulate propeller noise as transmitted into the aircraft cabin by the dominant airborne path, thereby enabling a parametric study of synchrophasing to be performed. The information acquired was then used to define the characteristics of synchrophasing and to evaluate the potential propeller noise reduction. Hence, this experimental investigation has led to a better understanding of the synchrophasing concept and the mechanisms of sound transmission into aircraft cabins.

This experimental investigation is being done in conjunction with an analytical investigation.[4]

Experimental Setup and Procedure

The experimental setup is presented in Fig. 1. The aircraft fuselage was modeled as a finite unstiffened aluminum cylinder 0.508 m in diameter and 1.245 m long. The cylinder was formed from a 1.63-mm-thick aluminum sheet and has an epoxy-bonded butt-joint seam with a 5-mm-wide exterior strap. Future investigations will involve studying the effects of more complex cylinder geometries; however, the purpose of this paper is to present preliminary results. The cylinder is sealed at both ends with 1.9-cm-thick wooden end caps and is freely supported at the ends.

The noise disturbances due to the propellers were modeled initially as monopole sources. Each monopole source is composed of a pair of 60-W University Sound driver units. Extension tubes are attached to the driver units for the purpose of bringing the driver exits closer together thereby enabling the pair of drivers to more closely approximate a point source. By using two driver units instead of one, source levels can be increased enough to eliminate most signal-to-noise-ratio problems. In addition, this will enable the pair of

Presented as Paper 84-2370 at the AIAA/NASA Ninth Aeroacoustics Conference, Williamsburg, VA, Oct. 15-17, 1984; received Nov. 20, 1984; revision received Aug. 9, 1985.

*Instructor, Mechanical Engineering. Student Member AIAA.
†Associate Professor, Mechanical Engineering.

drivers to be used as a dipole source for future investigations. A monopole source was mounted on each side of the cylinder at the axial centerline to simulate the noise disturbances due to the propellers. The source height could be varied to study the effect of asymmetric loading on synchrophasing; however, for this investigation both source heights were fixed at the vertical centerline of the cylinder. The sources were rigidly mounted to the grated floor of the anechoic chamber such that the ends of the extension tubes are 10.8 cm from the cylinder. To simulate free-field conditions, the experiments were performed in a $2.3\times2.6\times4$ m anechoic chamber which has a low-frequency cutoff of 250 Hz.

A schematic diagram of the experimental setup showing model details and microphone locations is presented in Fig. 2. Three 6-mm-diam B&K condensor microphones were mounted on an interior traversing mechanism at radial positions $r/a=0.150$, 0.513, and 0.925. The microphone cables were passed through a hole in one of the wooden end plates, which was subsequently sealed with modeling clay. These three microphones were used to evaluate the axial, radial, and circumferential pressure distributions inside the cylinder. Another 6-mm-diam B&K condenser microphone was used to measure the axial and circumferential pressure distributions on the exterior of the cylinder. In addition, two 6-mm-diam B&K condenser microphones were positioned 5.4 mm directly in front of the two monopole sources and were used to set the amplitude and relative phase (i.e., synchrophase angle) of each source.

A schematic diagram of the data acquisition system is presented in Fig. 3a. All microphone signals were conditioned with B&K signal conditioners and amplified and filtered of low-frequency noise with Ithaco amplifiers before being fed into a switching box. Nine B&K accelerometers were mounted equally spaced around the circumference of the cylinder in the propeller plane ($x/a=0.0$) to measure the modal response of the shell due to source excitation. The accelerometer signals were conditioned and fed into the switching box. Because it is necessary to locate both signal conditioners in the anechoic chamber, the exterior walls of the signal conditioner boxes were lined with a 12.7-mm-thick flexible polyurethane polyester foam to reduce acoustic scattering. All of the microphone and accelerometer signals were processed in turn with a two-channel Zonic 5003 fast fourier transformer (FFT). The cutoff frequency was set to 1500 Hz, giving a frequency bandwidth of 7.3 Hz. A phase meter and oscilloscope were used to monitor the amplitudes, relative phase, and waveforms of the signals from the source microphones. The oscilloscope was also used to monitor the remaining microphone and accelerometer signals for distortions and clipping before data acquisition was initiated.

A schematic diagram of the source generation system is presented in Fig. 3b. The reference pure tone signal for the noise source was generated by a Wavetek function generator and was monitored by a Hewlett-Packard frequency counter. The reference signal was fed into a four-channel gain-phase board where the gain and phase of the first two channels were set based upon the signals from the source microphones. The signals from the gain-phase board were then amplified and sent to the monopole sources. A digital voltmeter was used to monitor the output voltages of the amplifiers to ensure that the sources were not being overloaded.

The interior microphones were initially positioned horizontally in the source plane toward source I (i.e., $x/a=0.0$, $\theta=0$ deg) as shown in Fig. 2. Pressure measurements were recorded for the three radial microphone stations over the range of synchrophase angles of $\phi=0$-360 deg, using 45-deg phase increments. Additional pressure measurements were recorded at 5-deg increments around the optimum synchrophase angle of each interior microphone. While in the propeller plane, this procedure was repeated in the upper half of the cylinder at four additional circumferential positions—$\theta=45$, 90, 135, and 180 deg. This procedure was also repeated in the horizontal source plane (at $\theta=0$ deg) at axial

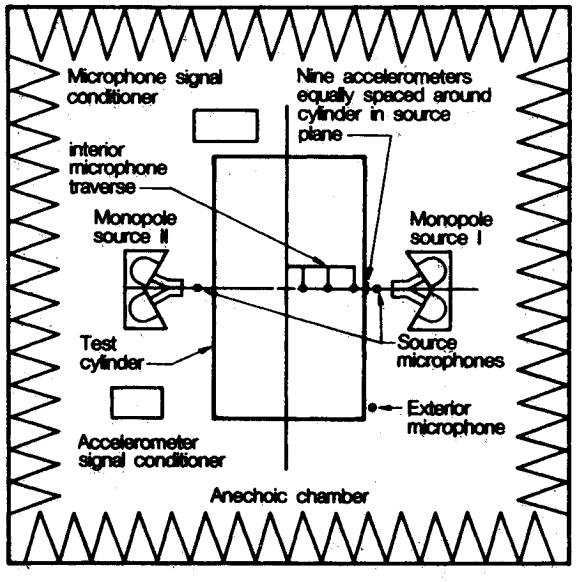

Fig. 2 Schematic diagram of experimental setup.

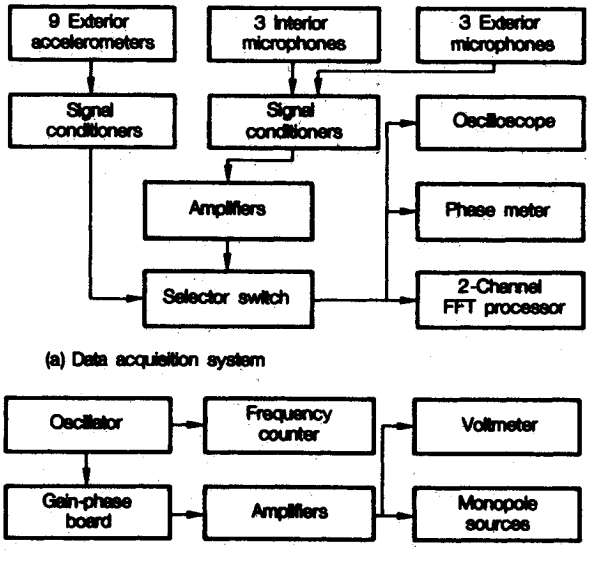

Fig. 3 Schematic diagram of instrumentation.

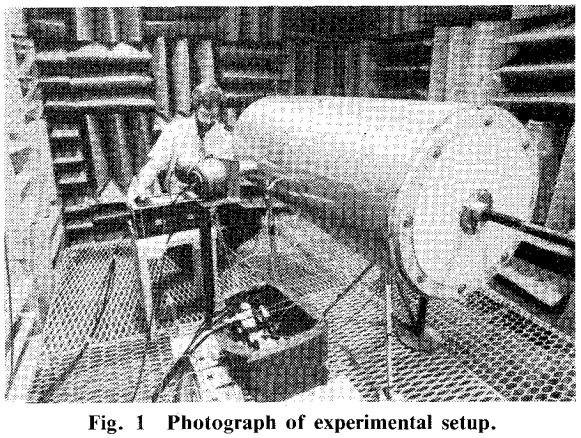

Fig. 1 Photograph of experimental setup.

positions $x/a=0.4$, 0.8, and 1.6. Exterior microphone measurements were recorded at 15 axial positions in the horizontal source plane (at $\theta=0$ deg) for synchrophase angles of $\phi=0$ and 180 deg. Finally, exterior microphone measurements were recorded in the propeller plane at seven circumferential positions for synchrophase angles of $\phi=0$ and 180 deg. All measurements were completed for pure tone source conditions of 680 and 708 Hz. These frequencies were chosen because they correspond to typical scaled fundamentals of the propeller noise. A third case was run with the source conditions again set to 708 Hz. However, for this case, a layer of 12.7-mm-thick flexible polyurethane polyester foam was placed on the interior of the cylinder covering 145 deg of the bottom of the cylinder.

Modal Decomposition of Shell Vibration

The radial vibration response of the cylinder was measured for the modal decomposition algorithm. The relative amplitudes and phases of the nine equally spaced accelerometers were measured over a range of synchrophase angles from $\phi=0$ to 360 deg, using 45-deg phase increments. Results from the decomposition algorithm defined the relative modal composition of the cylinder, thereby enabling the dominant mode of the cylinder to be determined for various synchrophase angles. The modal composition of the vibrational response of the cylinder is an essential element in understanding how sound is transmitted into the model.

The decomposition technique used in this investigation is similar to methods proposed by Moore[5] and Silcox and Lester.[6] The radial displacement of a cylinder at any given time can be represented by a Fourier series of sines and cosines as follows.

$$w(\theta,t)=\sum_{n=0}^{\infty}\left[A_n\cos(n\theta)+B_n\sin(n\theta)\right]e^{j\omega t} \tag{1}$$

When a cylinder is excited, circumferential waves propagate in both directions around the cylinder combining to create an interference pattern or standing wave. To solve for the complex modal amplitudes A_n and B_n, Eq. (1) is multiplied by $\cos(m\theta)$ and $\sin(m\theta)$, respectively, and integrated from 0 to 2π. Thus,

$$\int_0^{2\pi} w(\theta)\cos(m\theta)\,d\theta=\sum_{n=0}^{\infty}\left[\int_0^{2\pi} A_n\cos(n\theta)\cos(m\theta)\,d\theta+\int_0^{2\pi} B_n\sin(n\theta)\cos(m\theta)\,d\theta\right] \tag{2}$$

$$\int_0^{2\pi} w(\theta)\sin(m\theta)\,d\theta=\sum_{n=0}^{\infty}\left[\int_0^{2\pi} A_n\cos(n\theta)\sin(m\theta)\,d\theta+\int_0^{2\pi} B_n\sin(n\theta)\sin(m\theta)\,d\theta\right] \tag{3}$$

where $m=0,1,2,3,\ldots,\infty$ and the time dependence $e^{j\omega t}$ has been omitted. By utilizing the orthogonality characteristics of the Fourier series, Eqs. (2) and (3) can be reduced and rearranged to solve explicitly for the modal amplitudes. The resulting equations are

$$A_n=\frac{1}{\epsilon\pi}\int_0^{2\pi} w(\theta)\cos(n\theta)\,d\theta \tag{4}$$

$$B_n=\frac{1}{\epsilon\pi}\int_0^{2\pi} w(\theta)\sin(n\theta)\,d\theta \tag{5}$$

where

$\epsilon=2$ for $n=0$ and $\epsilon=1$ for $n>0$; $n=0,1,2,3,\ldots,\infty$

If $w(\theta)$ is known completely as a function of θ, all of the modal amplitudes can be determined. In practice, however, $w(\theta)$ is known only at discrete points around the cylinder. Therefore, the integrals of Eqs. (4) and (5) can be represented as Fourier summations of the form

$$A_n=\frac{1}{\epsilon\pi}\sum_{p=1}^{N_p} w(\theta_p)\cos(n\theta_p)\Delta\theta_p \tag{6}$$

$$B_n=\frac{1}{\epsilon\pi}\sum_{p=1}^{N_p} w(\theta_p)\sin(n\theta_p)\Delta\theta_p \tag{7}$$

where N_p is the number of circumferential positions where measurements are acquired and $\Delta\theta_p=2\pi/N_p$ for equally spaced measuring points. In essence, the summation is an approximation to the integral but since the sine and cosine functions are periodic and the integration is done over one period, the error cancels out. However, this is true only if the number of the highest order mode generated is less than or equal to $N_p/2$ (Nyquist criteria). In addition, if one of the measuring points is positioned on a node the number of measuring points is reduced by 1, as no information is acquired at this position.

In practice, the assumed mode shapes are fitted to the measured points so that measurement errors or contributions from modes excluded from the decompositions may cause serious errors in the results of the decomposition. As long as the contributions from the dominant modes are included in the decomposition, the errors due to higher order modes are negligible. One method to check the decomposition results is to regenerate the radial displacements by substituting the modal amplitudes from the decomposition back into the Fourier series. A reproduction of the measured radial displacements gives credibility to the decomposition results.

In practice, the modes excited most effectively are the $n=1$ and 2 modes. Therefore, the highest order mode decomposed for this investigation was limited to the $n=4$ mode. Thus, nine equally spaced measuring points were used in this investigation. This ensures that there are at least enough measuring points off nodal positions to decompose five modes.

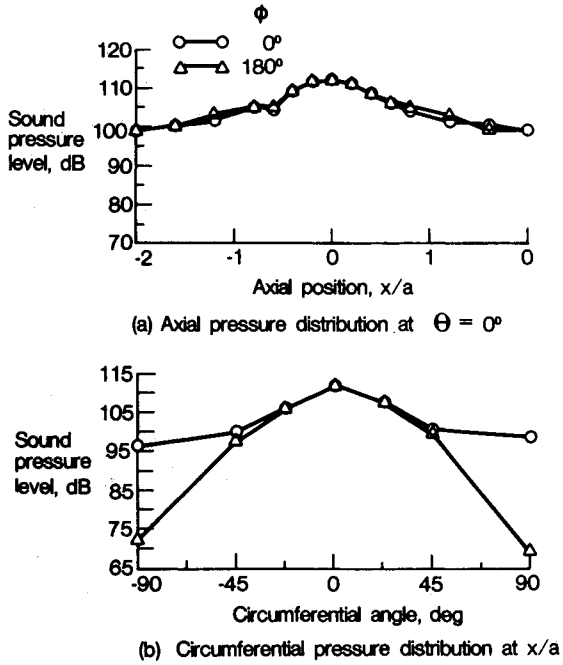

Fig. 4 Exterior pressure measurements of cylinder for $f=680$ Hz.

Results and Discussion

The results presented herein are from the case with pure tone source conditions of 680 Hz. This case was chosen because it clearly defines the basic characteristics of synchrophasing.

Figure 4 shows a comparison of the axial and circumferential pressure distributions on the exterior of the cylinder for synchrophasing angles of $\phi = 0$ and 180 deg. Although propeller sources are better modeled as dipoles, the axial and circumferential pressure distributions of the exterior of the cylinder due to the monopole sources used in this investigation are surprisingly similar to those measured on the external of an actual twin-engine turboprop aircraft fuselage.[7] The axial pressure distribution on the exterior of the cylinder is symmetric about the propeller plane and decays about 13 dB by two cylinder radii. The similarity between this result and those from Ref. 7 implies that the pressure forcing function at the fuselage surface is due to the near field of each source or a very directional source. The synchrophase angle appears to have a negligible effect on the axial pressure distribution at $\theta = 0$ deg. However, the synchrophase angle has a significant effect on the circumferential pressure distribution for $\theta > 45$ deg. This indicates that the near field of the source has substantially decayed in this region, thereby allowing diffraction effects around the cylinder to become important. The circumferential pressure distribution is symmetric about the horizontal source plane and decays 13-16 dB for a synchrophase angle of $\phi = 0$ deg, and 40-42 dB for a synchrophase angle of $\phi = 180$ deg. The more rapid decay in the circumferential pressure distribution for a synchrophase angle of $\phi = 180$ deg can be explained using an interference interpretation. Near a point of symmetry between the sources (i.e., $\theta = 90$ deg), cancellation occurs as the contribution from each source is relatively equal. However, in a region near $\theta = 0$ or 180 deg the contribution from each individual source dominates the exterior pressure field and the synchrophase angle has little effect.

Figure 5 shows the relative circumferential modal amplitudes of the cylinder vs synchrophase angle in the propeller plane for modes $n = 0$-4. The modal response of the cylinder is dominated by the $n = 2$ circumferential mode. For an ideal cylinder with the sources symmetrically positioned, as shown in Fig. 2, the B_n modes should theoretically be zero. However, the decomposition results show significant B_n modes with the $n = 2$ mode dominating. The presence of significant B_n modes is most likely caused by cylinder asymmetry or the presence of the butt-joint seam along the cylinder leading to a coupling effect with the A_n modes. The cylinder imperfections significantly alter the modal composition of the cylinder and the contained acoustic field, and, therefore, will affect the results of this experimental investigation. These results illustrate the need for cylinder vibration monitoring to be carried out in conjunction with interior pressure measurements in order to successfully explain the resultant effects.

All of the modal amplitudes peak for a synchrophase angle of $\phi = 45$ deg, and generally decrease to a minimum near a synchrophase angle of $\phi = 180$ deg. The results of the decomposition were checked by back substituting the modal amplitudes into the Fourier series. Results showed that there was a $< 0.1\%$ difference between the amplitudes and phases of the measured and reproduced radial displacements, thereby giving credibility to the decomposition results.

Figure 6 shows the interior pressure measurements vs synchrophase angles measured in the propeller plane at the three radial microphone stations for a circumferential position of $\theta = 0$ deg. The potential noise reduction varies from 15 to 25 dB depending on radial position. The optimum synchrophase angles for the three radial stations are all near $\phi = 180$ deg. However, there is a slight variation in the optimum synchrophase angle with radial position.

The results from Fig. 6 can be explained by considering the radial vibration response of the shell. The monopole sources excite a series of circumferential modes in the shell

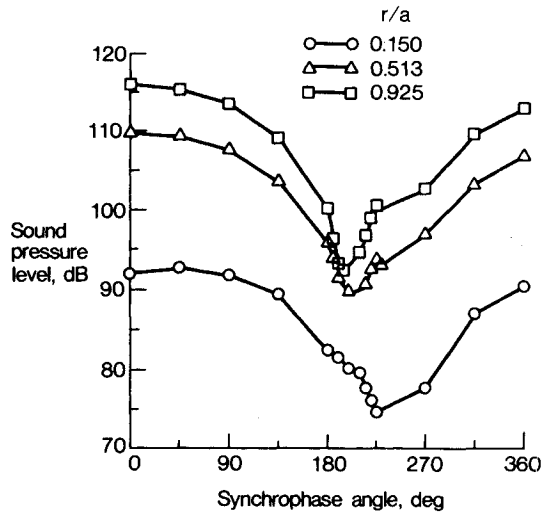

Fig. 6 Interior pressure measurements at $x/a = 0.0$, $\theta = 0$ deg, and $f = 680$ Hz.

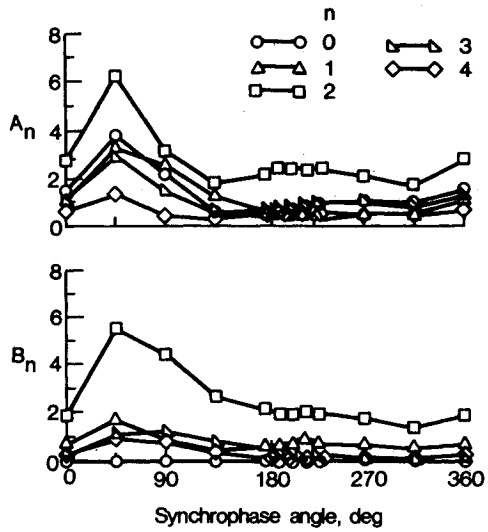

Fig. 5 Relative modal amplitudes of the cylinder at $x/a = 0.0$ and $f = 680$ Hz.

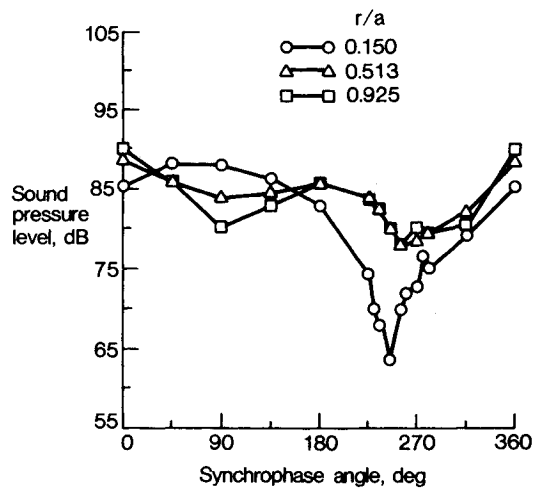

Fig. 7 Interior pressure measurements at $x/a = 0.0$, $\theta = 45$ deg, and $f = 680$ Hz.

wall which, in turn, couples to the contained acoustic field to govern the interior pressure distribution. Therefore, the total acoustic pressure at a given interior position is a superposition of acoustic pressures due to each circumferential mode generated in the cylinder. Theoretically, the optimum synchrophase angle to reduce the contributions from the even A_n modes and odd B_n modes is $\phi = 180$ deg. Similarly, the optimum synchrophase angle that reduces the contributions from the odd A_n modes and even B_n modes is $\phi = 0$ deg. The dominant mode generated in the 680-Hz case is the $n = 2$ mode with significant contributions coming from the $n = 0$, 1, and 3 modes. At circumferential positions $\theta = 0$ deg, the contributions to the interior pressure levels from the B_n modes are theoretically zero. With the dominant A_n mode being even (i.e., $n = 2$), this implies that the optimum synchrophase angle should be near $\phi = 180$ deg, as shown in Fig. 6. The small deviation from the expected optimum synchrophase angle of $\phi = 180$ deg is due to the odd A_n modes generated, which contribute somewhat to interior pressure distribution. In addition, asymmetry in the shell will cause some minor contributions from the B_n modes due to corresponding asymmmetry of the contained acoustic field. The variation of the optimum synchrophase angle with radial position is due to differing contributions from the circumferential modes at the different radial positions.

The interior pressure levels at $\theta = 0$ deg are very sensitive to the synchrophase angle. This is true even near the cylinder wall at $r/a = 0.925$. However, as shown in Fig. 4a, the exterior pressure distribution at $\theta = 0$ deg is essentially unaffected by the synchrophase angle. This result indicates that sound is not being transmitted directly into the cylinder via a localized area of the wall but instead excites a series of circumferential modes which subsequently couple to the interior acoustic field. Thus, the representation of an aircraft fuselage as a finite flat plate or curved panel may be inadequate at low frequencies.

Figure 7 shows the interior pressure measurements vs synchrophase angle measured in the propeller plane at the three radial microphone stations for a circumferential position of $\theta = 45$ deg. The potential noise reduction is about 10 dB for radial stations $r/a = 0.513$ and 0.925, and about 23 dB for $r/a = 0.150$. The optimum synchrophase angles for all three radial stations increase to near $\phi = 260$ deg. At $\theta = 45$ deg, contributions from all of the decomposed A_n and B_n modes will be present except for the A_2 and B_4 modes. This results in approximately equal contributions from modes with optimum synchrophase angles of $\phi = 180$ and 0 deg (or 360 deg). Therefore, an optimum synchrophase angle of 260 deg is not surprising. Due to a lack of dominance of modes with an optimum synchrophase angle of either $\phi = 0$ or 180 deg, the potential noise reduction by the synchrophasing technique has decreased significantly for radial stations $r/a = 0.513$ and 0.925. The $n = 0$ mode is the only mode that theoretically contributes to the acoustic pressure at the cylinder's centerline. Therefore, as the cylinder's centerline is approached, the $n = 0$ mode will begin to dominate and the decrease in the potential noise reduction is not observed for radial station $r/a = 0.150$.

Figure 8 shows the interior pressure measurements vs synchrophase angle measured in the propeller plane at the three radial microphone stations for a circumferential position of $\theta = 90$ deg. The potential noise reduction varies between 12-34 dB depending on radial position. The optimum synchrophase angle is $\phi = 180$ deg for radial stations $r/a = 0.513$ and 0.925, and $\phi = 0$ deg for $r/a = 0.150$. All of the modes that have an optimum synchrophase angle of $\phi = 0$ deg theoretically do not contribute to the interior acoustic field at $\theta = 90$ deg. Therefore, large potential noise reductions are expected with optimum synchrophase angles of $\phi = 180$ deg. Hence, the results at radial station $r/a = 0.150$ are quite surprising and difficult to explain. Apparently, the contributions from both A_n and B_n modes as well as imperfections in the cylinder combine to cause this unexpected result at $r/a = 0.150$.

As shown in Figs. 6-8 the interior pressure levels in the propeller plane are generally greatest near the shell wall and decrease rapidly as the centerline of the cylinder is approached. The low-pressure levels near the centerline of the cylinder ($r/a = 0.150$) are a result of the fact that the contributions to the interior acoustic field from all the modes, except the $n = 0$ mode, theoretically go to zero as the centerline of the cylinder is approached. Therefore, the pressure measurements at $r/a = 0.150$ are expected to be significantly lower than the other radial positions. This result gives additional support to the theory that the modal composition of the cylinder governs the interior acoustic field.

Figure 9 shows the interior pressure measurements vs synchrophase angle measured in the propeller plane at $r/a = 0.925$ for circumferential positions of $\theta = 0$, 45, 90, 135, and 180 deg. The interior pressure measurements vs synchrophase angle for $\theta > 90$ deg vary as a mirror image of the results for $\theta < 90$ deg, except that the pressure levels for $\theta > 90$ deg are about 8-13 dB lower than the pressure levels for $\theta < 90$ deg. The nonsymmetric circumferential pressure distribution is caused by the presence of significant B_n modal amplitudes due to the imperfections in the shell. Similar results were found at the radial stations $r/a = 0.150$ and 0.513.

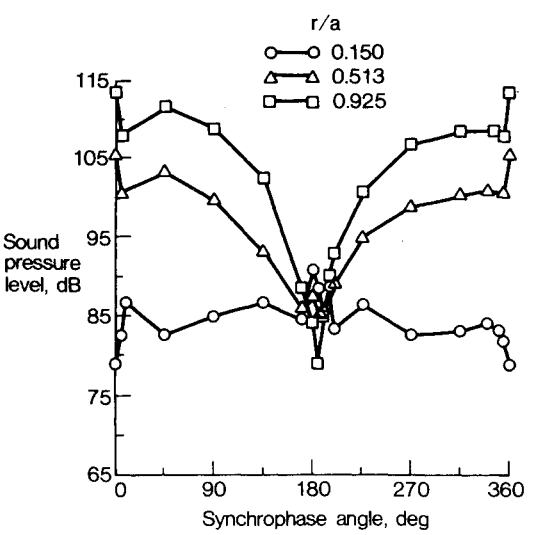

Fig. 8 Interior pressure measurements at $x/a = 0.0$, $\theta = 90$ deg, and $f = 680$ Hz.

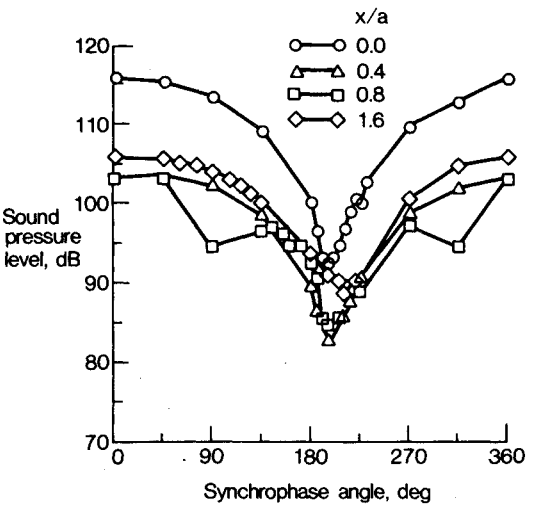

Fig. 9 Interior pressure measurements at $x/a = 0.0$, $r/a = 0.925$, and $f = 680$ Hz.

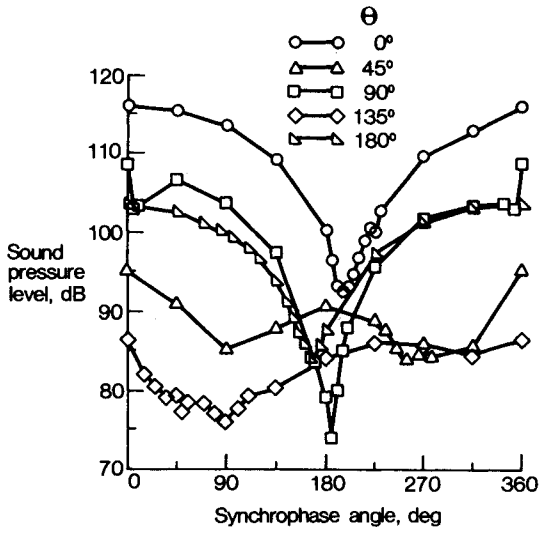

Fig. 10 Interior pressure measurements at $\theta=0$ deg, $r/a=0.925$, and $f=680$ Hz.

Figure 10 shows the interior pressure measurements vs synchrophase angle measured at $\theta=0$ deg for $r/a=0.925$ and axial positions $x/a=0.0$, 0.4, and 0.8, and 1.6. The interior pressure levels are very high in the propeller plane and decay rapidly with increasing axial position. This result is surprising for a finite cylinder and implies that the interior acoustic field is dominated by a near field in the propeller plane. The slight increase in the pressure levels at $x/a=1.6$ is a result of a second peak in the axial standing wave. However, this standing-wave peak is significantly lower than the dominant peak in the propeller plane. Thus, even for the finite unstiffened cylinder used in this experimental investigation, the majority of the acoustic energy is located in the shell in a localized region near the propeller plane.

The results of Figs. 4a and 10 show that the axial shell insertion loss (or noise reduction) varies dramatically with synchrophase angle. Thus, stabilization of the relative rotational phase of each propeller is essential before meaningful interior noise measurements can be obtained. The insertion loss presented by the shell wall is also physically interpreted better as a loss due to the modal response of the whole continuous cylinder surface rather than an attenuation due to a flat plate.

Although an infinite shell model with dipole sources is used in the analytical investigation of Ref. 4, the predicted synchrophasing characteristics are nearly identical to those obtained in this experimental investigation. The analytical exterior axial and circumferential pressure distributions are similar to those presented in Fig. 4 even though dipoles were used to model the propeller sources instead of monopoles. The optimum synchrophase angle and degree of attenuation from the analytical investigation closely resemble the results presented here for the various interior microphone positions. Also, the analytical interior pressure distribution at $\theta=0$ deg was found to be very sensitive to the synchrophase angle, while the exterior pressure distribution was unaffected by the synchrophase angle. Similar experimental results are shown in Figs. 4a and 10. The analytical interior acoustic field was dominated by a near field in the source plane implying that the majority of acoustic energy is located in the shell in a localized area near the propeller plane. Surprisingly, similar results were obtained from this experimental investigation even though a finite shell was used. This outcome implies that the end caps have a negligible effect on the interior acoustic field near the source plane. Thus, the results of this experimental investigation substantiate the assumptions of the infinite shell model used in Ref. 4.

Concluding Remarks

A simplified model of an aircraft fuselage was used to perform an experimental investigation of synchrophasing. The basic characteristics of synchrophasing have been defined. Potential noise reductions of 10-34 dB were measured throughout the interior of the cylinder. The optimum synchrophase angle and the degree of attenuation vary with location and depend on the modal composition of the cylinder and the relative contribution from each of these modes due to coupling with the interior acoustic field. The interior acoustic field was found to be dominated by pressure levels near the propeller plane, thus implying that an infinite cylinder is a reasonable model of an aircraft fuselage.

A computer algorithm was developed to decompose the modal composition of the cylinder for a range of synchrophase angles. The decomposition algorithm was found to be an essential tool for investigating the mechanisms of sound transmission into the cylinder. Modal decomposition results suggest that transmission of low-frequency sound into aircraft cabins is governed by modal cylinder vibration rather than localized transmission. Also, the results indicate that the near-field or directional characteristics of propeller sources in a real aircraft strongly determine the nature of the transmission phenomena. Asymmetries in the cylinder were found to couple cylinder circumferential modes of vibration. Thus, any type of structural modification (i.e., internal floors, ribs, etc.) is suspected to strongly affect the sound transmission.

The aircraft fuselage model and experimental procedure utilized in this investigation have been shown to be very successful in defining the characteristics of synchrophasing and other interior noise effects, as well as giving insight into the mechanisms of sound transmission into aircraft cabins. The beginning of an experimental data base has been developed; however, further studies are needed to completely understand the synchrophasing concept as well as other interior noise effects. Possible future investigations include: studying the effects of multiple pure tones, the presence of an internal floor, asymmetric source loading, ribs, stiffeners, vibrational inputs at the wing attachments, internal damping, utilizing dipole sources instead of monopole sources to investigate the directional influence of sources, and investigations of trace velocity effects. Finally, by coupling the results of the experimental model with the simplified analytical model,[4] a complete understanding of synchrophasing can be achieved.

Acknowledgments

The authors are grateful to NASA's Langley and Lewis Research Centers for their support of this research under Grant NAG 1-390.

References

[1]Metzger, F. B., "Strategies for Aircraft Interior Noise Reduction in Existing and Future Propeller Aircraft," SAE Paper 81-0560, 1981.

[2]Johnston, J. F., Donham, R. E., and Guinn, W. A., "Propeller Signatures and Their Use," AIAA Paper 80-1035, 1980.

[3]Magliozzi, B., "Synchrophasing for Cabin Noise Reduction of Propeller-Driven Airplanes," AIAA Paper 83-0717, 1983.

[4]Fuller, C. R., "Noise Control Characteristics of Synchrophasing—An Analytical Investigation," AIAA Paper 84-2369, 1984.

[5]Moore, C. J., "Measurement of Radial and Circumferential Modes in Annular and Circular Fan Ducts," *Journal of Sound and Vibration*, Vol. 62, No. 2, 1979, pp. 235-256.

[6]Silcox, R. J. and Lester, H. C., "Sound Propagation Through a Variable Area Duct: Experiment and Theory," *AIAA Journal*, Vol. 20, Oct. 1982, pp. 1377-1384.

[7]Mixson, J. S., Barton, C. K., Piersol, A. G., and Wilby, J. F., "Characteristics of Propeller Noise on an Aircraft Fuselage Related to Interior Noise Transmission," AIAA Paper 79-0646, 1979.